Environmental Science & Technology

pubs.acs.org/est

Article

Maximum Removal Efficiency of Barium, Strontium, Radium, and Sulfate with Optimum AMD-Marcellus Flowback Mixing Ratios for Beneficial Use in the Northern Appalachian Basin

Bonnie McDevitt,* Michael Cavazza, Richard Beam, Eric Cavazza, William D. Burgos, Li Li, and Nathaniel R. Warner

Cite This: https://dx.doi.org/10.1021/acs.est.9b07072

Read Online

ACCESS | Metrics & More | Article Recommendations | Supporting Information

ABSTRACT: Mixing of acid mine drainage (AMD) and hydraulic fracturing flowback fluids (HFFF) could represent an efficient management practice to simultaneously manage two complex energy wastewater streams while reducing freshwater resource consumption. AMD discharges offer generally high sulfate concentrations, especially from the bituminous coal region of Pennsylvania; unconventional Marcellus shale gas wells generally yield HFFF enriched in alkali earth metals such as Sr and Ba, known to cause scaling issues in oil and gas (O&G) production. Mixing the two waters can precipitate HFFF-Ba and -Sr with AMD-SO_4, therefore removing them from solution. Four AMD discharges and HFFF from two unconventional Marcellus shale gas wells were characterized and mixed in batch reactors for 14 days. Ba could be completely removed from solution within 1 day of mixing in the form $Ba_xSr_{1-x}SO_4$ and no further significant precipitation occurred after 2 days. Total removal efficiencies of Ba + Sr + SO_4 and the proportion of Ba and Sr in $Ba_xSr_{1-x}SO_4$ depended upon the Ba/Sr ratio in the initial HFFF. A geochemical model was calibrated from batch reactor data and used to identify optimum AMD−HFFF mixing ratios that maximize total removal efficiencies (Ba + Sr + SO_4) for reuse in O&G development. Increasing Ba/Sr ratios can enhance total removal efficiency but decrease the efficiency of Ra removal. Thus, treatment objectives and intended beneficial reuse need to be identified prior to optimizing the treatment of HFFF with AMD.

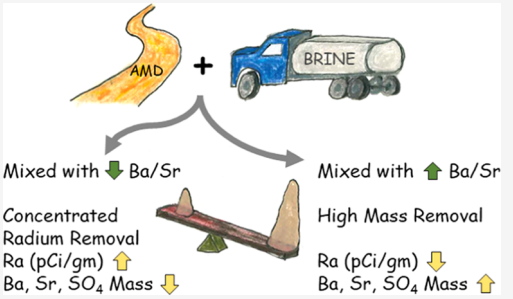

INTRODUCTION

The Appalachian Basin Marcellus and Utica shales represent two of the largest unconventional natural gas reservoirs in the United States with approximately 906 million m^3 per day of natural gas production.[1] Pennsylvania alone accounted for approximately 16% of the United States' natural gas production in 2018.[2] More than 11 500 active unconventional wells have been drilled in Pennsylvania[3] in addition to an estimated 100 000−300 000 conventional wells. While presenting economic growth opportunities to mainly rural areas, shale gas extraction imposes significant strains on local freshwater resources as each unconventional well consumes between 8000 and 100 000 m^3 (2−13 million gallons) of water during well stimulation.[4] On a nationwide scale, approximately 90% of U.S. unconventional produced water, including hydraulic fracturing flowback fluid (HFFF), is disposed by injection, which has led to concerns regarding seismicity, spills, and local water stress in arid, semiarid, and even temperate regions such as Pennsylvania during low-flow or drought conditions.[5−9] Of the six largest U.S. shale regions, four (Bakken, Niobrara, Permian, and Eagle Ford) exhibit areas with extremely high baseline water stress (defined as >80%), while the Marcellus contains areas with high water stress (40−80%).[10] Of the water injected into the Marcellus or Utica, only 10−40% returns to the surface as the hydraulic fracturing flowback fluid (HFFF), here defined as the fluid that returns in the first 30 days of well production.[11] Extraction activities in the Appalachian Basin produce a complex wastewater brine (10−300 g/L total dissolved solids (TDS)), which contains high concentrations of hydrocarbons, trace and heavy metals, naturally occurring radioactive material (NORM), and significantly elevated concentrations of other alkaline-earth metals such as Ba and Sr, posing issues for surface water disposal to streams.[4,7,8,12−17]

Many of those same Pennsylvania streams have also experienced decades of acid mine drainage (AMD) due to abandoned coal mines and coal waste products, making AMD the second most persistent water quality problem in the state, second only to agriculture.[18] There are approximately 5600 abandoned coal mine sites in Pennsylvania that have impacted roughly 8850 km of streams, 1.5 km^2 of freshwater lakes, and in

Received: November 21, 2019
Revised: March 18, 2020
Accepted: March 20, 2020

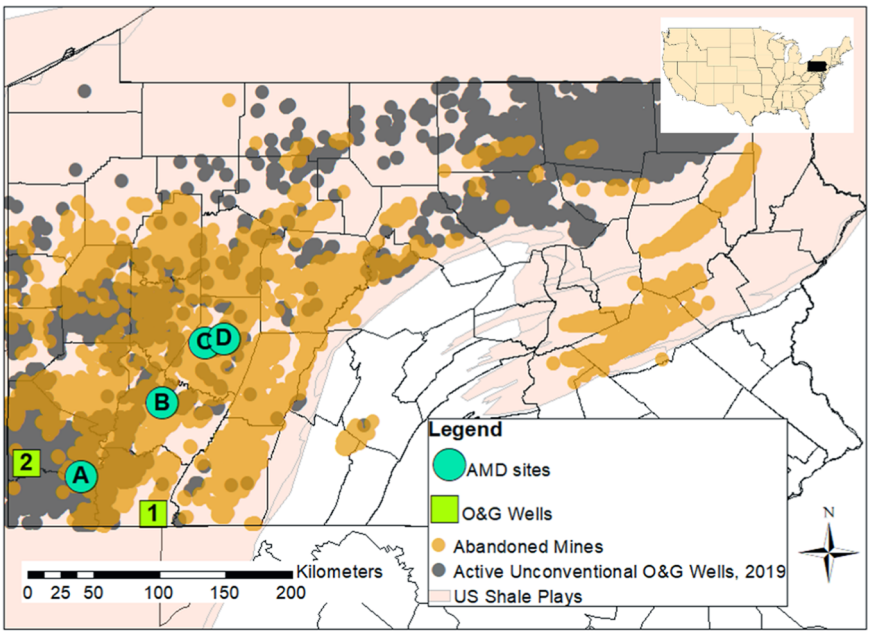

Figure 1. Map of abandoned mine sites and active unconventional O&G wells as of 2019 in Pennsylvania overlain by the Marcellus shale formation. AMD sites A−D are within the bituminous coal region. Unconventional Marcellus shale gas wells 1 and 2 were sampled during both early (E) and late (L) flowback periods.

2006 cost the state an estimated $108 million in recreational fishing losses alone.[18] Pennsylvania's Abandoned Mine Lands (AML) Program grants, derived from a fee on each ton of coal mined by the active mining industry to remediate priority sites, have not been sufficient to remedy the estimated $5−15 billion dollars in watershed damages.[18,19] Based on a recharge estimate of 0.3 m/year over 10 360 km^2 of mined land in Pennsylvania, total AMD discharges would equal 8633 million liters per day or a rough average of 1.5 million liters per day per site consistent with ranges of measured discharges.[20−22] AMD is typically characterized by low to neutral pH (3−7) due to sulfuric acid (H_2SO_4) leached from pyritic rocks, high concentrations of metals including iron, manganese, and aluminum, high conductivity, and relatively high concentrations of sulfate, depending on geologic locations.[20] Sulfate concentrations in bituminous coal mining regions (generally western Pennsylvania) have been reported to be higher than those of AMD in the anthracite region (generally eastern) of Pennsylvania.[20]

Due to the proximity of O&G extraction activities and AMD discharges in Pennsylvania, the use of AMD in place of local freshwater withdrawals poses a unique opportunity to repurpose AMD that otherwise pollutes local waterways.[23−25] Coonrod et al. (2020) proposes the closing of the hydraulic fracturing water cycle by encouraging "fit for purpose," flexible, and low-cost treatment technologies for industry reuse of unconventional produced water followed by recycling for alternative beneficial uses (i.e., agriculture, road deicing, and dust suppression).[26] The U.S. Environmental Protection Agency (EPA) and Department of Energy (DOE) are currently seeking alternative uses for O&G produced water for beneficial use, as commonly practiced in the western United States.[27−30] Sequestration of alkaline-earth metals from O&G wastewater including Ba, Sr, and Ra by sulfate mineral co-precipitation into barite ($BaSO_4$) and radiobarite (Ba,Ra)-SO_4 is widely reported and commonly utilized in produced water radium treatment prior to surface water disposal.[4,24,31−37] Less commonly reported but also effective in Ra and Sr sequestration is celestite ($SrSO_4$) and radiocelestite (Sr,Ra)SO_4 precipitation.[12,24,34,38] Direct use of untreated AMD with high SO_4 concentrations (previously proposed >100 mg/L SO_4) for hydraulic fracturing has the potential to promote mineral precipitate scaling downhole, causing reservoir clogging and decreasing O&G extraction efficiencies, leading to industry trepidation regarding the process.[39−41] However, if AMD and produced water are blended at the surface prior to injection into the O&G formation, mineral precipitates would be allowed to form, settle, and be removed from the bulk fluid, allowing this wastewater recycle stream to be a viable and sustainable process.[25] Previous studies have focused on the removal of SO_4, Ba, and Ra through the formation of the thermodynamically favorable (Ba,Ra)SO_4 with less focus on ($SrSO_4$) or (Sr,Ra)SO_4 due to slower precipitation rates for use in field-scale treatment.[23,24,42] Those same studies confirmed the formation of $Ba_xSr_{1-x}SO_4$ minerals but did not explore in depth the initial mixing conditions and volumetric mix ratios that led to varying compositional proportions—important for predicting total ion removal efficiencies (Ba + Sr + SO_4) for treatment. Additionally, previous studies lacked quantitative guidance for optimum mixing of various input fluids and proposed future studies with longer duration to confirm that significant precipitation does not occur beyond a maximum of 48 h of mixing.

This work addresses this knowledge gap by (1) characterizing the formation of $Ba_xSr_{1-x}SO_4$ with wide-ranging AMD−HFFF volumetric mix ratios and 14 day experiments and (2) developing a geochemical code based on experimental data to predict the formula of precipitates and extrapolating the data to wider mixing conditions for any volumetric mix ratio. Laboratory batch experiments were used to calibrate the model (CrunchFlow) to identify mixing ratios of AMD−HFFF that maximize total removal efficiencies of Ba + Sr + SO_4. Finally, this study fills a knowledge gap by (3) identifying the importance of the initial AMD−HFFF mix Ba/Sr molar ratio

https://dx.doi.org/10.1021/acs.est.9b07072
Environ. Sci. Technol. XXXX, XXX, XXX−XXX

Table 1. Field Sampling and Laboratory Analysis for Major Ions from the Four AMD Sites (A−D) and Marcellus Shale Gas Wells 1 and 2 during Both Early (E) and Late (L) HFFF Sampling

		A	B	C	D	1 E	1 L	2 E	2 L
Location		Clyde	Crabtree	Ernest	Tanoma	Well 1 (E)[a]	Well 1 (L)[b]	Well 2 (E)	Well 2 (L)
Flowrate	L/min	3,785	27,959	6,677	11,474	-	-	-	-
pH	s.u.	6.3	5.9	5.4	6.7	6.2	6.4	6.1	6.2
Alkalinity	mg/L	335	142	20	185	256	218	63	86
Na	mg/L	1,860	120	87	85	24,790	25,880	35,400	39,500
Ca	mg/L	301	165	101	81	6,204	8,244	13,300	15,400
Mg	mg/L	108	47	24	20	626	841	1,308	1,616
Ba	mg/L	0.02	0.02	0.03	0.03	3,040	4,590	539	728
Sr	mg/L	ND[c]	1.2	1.0	1.3	1,400	1,980	2,630	3,320
Fe	mg/L	0.03	61	12	5	120	198	42	55
Cl	mg/L	836	73	57	10	56,025	60,357	91,939	103,061
SO_4	mg/L	3,873	614	448	293	262	ND	78	ND
TOC	mgC/L	-	-	-	-	180	87	33	21
^{226}Ra	pCi/L	-	-	-	-	-	883	-	1,012
^{228}Ra	pCi/L	-	-	-	-	-	31.5	-	15.6

[a] E denotes early HFFF
[b] L denotes late HFFF
[c] Not detected
(-) Not measured

Table 2. Summary of Volumetric Mix Ratios in the 14 Day Batch Experiments[a]

	SO_4:Ba + Sr	SO_4:Ba	AMD	HFFF	barite	celestite	Ba	Sr	SO_4	total[a]	Ra-228	Ra-226
mixture	molar	molar	vol %	vol %	SI	SI	removal (%)	removal (%)	removal (%)	removal (%)	removal (%)	removal (%)
A + IE	0.98	1.69	49	51	3.7	0.0	100	53	74	80	–	–
A + 2E	0.93	8.04	46	54	2.8	0.1	100	46	53	54	–	–
A + $1L^T$	1.24	2.09	60	40	3.9	0.1	100	41	73	78	–	–
A + $2L^T$*	4.14	32.84	81	19	3.0	0.2	100	48	4	14	87	100
B + IE	1.05	1.81	86	14	3.0	−0.7	100	32	62	71	–	–
B + 2E	1.00	8.65	84	16	2.1	−0.6	100	18	24	28	–	–
B+ $1L^T$	1.43	2.41	91	9	3.1	−0.7	100	14	56	64	100	100
B+ $2L^T$	0.20	1.61	54	46	2.3	−0.5	73	0	100	9	–	–
C + IE	1.23	2.13	89	11	3.1	−0.7	100	30	60	69	–	–
C + 2E	1.18	10.24	88	12	2.1	−0.7	99	15	30	30	–	–
C + $1L^T$	1.30	2.19	91	9	3.1	−0.7	100	22	51	63	–	–
C + $2L^T$	0.15	1.21	51	49	2.2	−0.6	70	0	100	15	82	82
D + IE	1.14	1.97	93	7	2.7	−1.1	100	37	62	71	–	–
D + 2E	1.09	9.49	92	8	1.8	−1.0	93	8	19	20	–	–

[a]Initial barite and celestite SI were included for mixtures as well as removal efficiencies for Ba, Sr, SO_4, and total (Ba + Sr + SO_4) at the end of the experiment. Ra-226 and -228 removal were only measured in three samples. [b][a] Ba + Sr + SO_4 removal. [T]Time-course mixtures sampled 0−14 days. * Ratio to achieve 1:1 mol equiv SO_4Ba + (4*Sr). (−) Not analyzed.

with regards to treatment agenda and wastewater management decisions for either optimum Ba + Sr + SO_4 and/or Ra removal.

MATERIALS AND METHODS

AMD and HFFF Liquid Characterization. Water samples were collected and flowrates were measured in Spring and Fall 2015 from four AMD discharges in Pennsylvania (identified as A−D; Figure 1).

Two unconventional Marcellus shale gas wells located in southwest Pennsylvania were sampled in Fall 2015 during both early (E) (day 1−2) and late (L) (day 30) flowback periods to yield four samples for testing (identified as 1E, 1L, 2E, and 2L). The four HFFF samples were stored up to 2 weeks at ambient temperatures until mixing to mimic expected field conditions (e.g., storage in open ponds or tanks). The four AMD sites were selected because, collectively, their geochemical characteristics represent the bituminous coal region of southwest Pennsylvania. Previous sampling data narrowed viable AMD discharges to the bituminous coal region due to higher SO_4 concentrations.[43,44] Specific conductance, pH, temperature, and ORP were measured in the field at each location. Water samples were field-filtered with 0.45 μm cellulose acetate membrane filters and preserved with nitric acid (pH ≤ 2) for cation and trace metal analyses. Following filtration and preservation, samples were stored in a refrigerator at 4 °C in the laboratory prior to analysis. Raw AMD bulk water samples, like HFFF bulk water samples, were stored for up to 2 weeks at ambient temperatures until mixing. Chloride and sulfate concentrations were analyzed by colorimetry via

https://dx.doi.org/10.1021/acs.est.9b07072
Environ. Sci. Technol. XXXX, XXX, XXX−XXX

the standard method 4500 Cl-E automated ferricyanide method and EPA method 375.2, respectively. Alkalinity was analyzed by titration. Cations and trace metals were analyzed by inductively coupled plasma mass spectroscopy (ICP-MS). All sample data analyzed were within 10% charge balance between cations and anions for quality assurance. Ions of importance to the study are presented in Table 1, while complete datasets for AMD and HFFF samples are included in the Supporting Information (Tables S1 and S2). Radium 226 and 228 were measured in the HFFF samples 1L and 2L and in three samples collected after the 14 day batch reaction period. Radium 226 was analyzed by radon emanation using EPA method 903.1, and radium 228 was analyzed using the Brooks−Blanchard method by precipitation of barium and lead sulfate, purification, and β counting. Total organic carbon (TOC) was measured on HFFF samples on a Shimadzu TOC-VCPH TOC analyzer.

Batch Mixing Experiments. All batch mixing experiments were conducted by combining different volumetric ratios of AMD samples with HFFF samples in 5-gallon plastic containers at 25 °C using raw unfiltered samples (n = 14 mix ratios) (Table 2). Volumetric mixing ratios of AMD and HFFF were calculated to achieve specific initial saturation index (SI) values for barite and celestite (SI = log(ion activity product[IAP]/K_{eq})), according to reactions detailed in Table S3.

The majority of experiments were designed to provide 1:1 molar ratios of sulfate to barium plus strontium (SO_4:Ba + Sr), assuming no other reactions, for stoichiometric removal of barium and strontium. While some AMD−HFFF mixtures were slightly enriched in sulfate (e.g., A + 1L), others had only enough sulfate to form barite but not celestite (e.g., A + 2E). All barite SI values were higher under each mixing condition compared to celestite SI values, indicating the favorability of barite-driven precipitation. Some celestite SI values were near equilibrium or even <0. The sulfate concentrations of the AMD samples and the Ba + Sr concentrations of the HFFF samples dictated the volumetric mixing ratios used for the different experiments. A + 1E and A + 1L represented the highest barite SI values due to the highest sulfate concentrations, requiring among the least dilutions of HFFF with AMD (51%:49% and 60%:40%, respectively). In contrast, the low sulfate concentrations from D led to higher AMD volumes diluting HFFF so that 1:1 SO_4:Ba + Sr ratios were achieved (93%:7%). Removal efficiencies were calculated as the respective ratio of the individual or additive total mass removal of Ba, Sr, and SO_4 compared to the individual or additive total initial mass from the AMD−HFFF mixture, assuming conservative mixing of constituent solutions, according to

$$\left(1 - \frac{C_f}{C_0}\right) \times 100$$

where C_f represents the final concentration of the mixture and C_0 represents the initial concentration of the mixture.

A subset of batch mixing experiments was designed to provide initial SO_4:Ba + Sr molar ratios that were far from 1:1. For these cases, SO_4:Ba + Sr molar ratios ranged from 0.15 to 4.14 (Table 2). These mixing experiments were used to calibrate the geochemical model to identify the optimum mixing ratios that maximize cation and sulfate removal. Three of the four AMD sites were selected for time-course mixing experiments (n = 6) based on high (A, 3873 mg/L), median (B, 614 mg/L), and low (C, 448 mg/L) sulfate concentrations. From these mixing experiments, water samples were collected from the batch reactors each day from 0 to 14 days. These ratios reflect a varying mix of AMD−HFFF to achieve both an approximate 1:1 mol equiv of SO_4:Ba + Sr (A + 1L, B + 1L, C + 1L) and an approximate 1:1 mol equiv of SO_4:Ba (B + 2L and C + 2L) to test if Ba or Ba + Sr controls precipitation. Experiment A + 2L mix ratio was targeted to achieve a 1:1 mol equivalent SO4:Ba + (4*Sr). Mixtures were analyzed for pH, alkalinity, Ba, Sr, Ca, and SO_4 by geochemical testing in Somerset, PA. Ra was measured after 14 days for A + 2L, B + 1L, and C + 2L.

From the time-course mixing experiments, batch reactors were decanted and precipitates were collected for mineralogical analysis (n = 6). Precipitates were oven-dried at 60 °C, pulverized for homogeneity, and analyzed on a PANalytical Empyrean X-ray diffractometer (XRD) and Jade software in the Materials Characterization Laboratory (MCL) at The Pennsylvania State University.

Geochemical Modeling with CrunchFlow. The reactive transport code CrunchFlow was set up to run in a reaction only (without transport) mode to simulate the laboratory batch mixing experiments.[45] In such systems without advective and diffusive transport, the code solves the following governing equation for the concentrations of independent primary species C_i

$$V\frac{\partial}{\partial t}(C_i) = \sum_{j=1,}^{nr} r_{i,j} = \sum_{j=1}^{nr} k_{i,j}A_j\left(1 - \frac{\mathrm{IAP}_j}{K_{\mathrm{eq},j}}\right),\ i = 1, 2, \ldots, np \quad (1)$$

where V is the total water volume of the batch reactor after mixing (L); the reaction rate $r_{i,j}$ (mol/s) is the jth mineral dissolution/precipitation reaction for species i following the transition state theory (TST) rate law; nr is the total number of mineral reactions that species i participates; $k_{i,j}$ is the kinetic rate constant (mol/m^2/s) for reaction j; A_j is the mineral surface area (m^2); IAP is the ion activity product (e.g., $a_{Ba^{2+}}a_{SO_4^{2-}}$ for barite reaction, where the activity is the product of activity coefficient and concentration); and $K_{eq,j}$ is the equilibrium constant of reaction j. The term $\mathrm{IAP}_j/K_{eq,j}$ quantifies the extent of disequilibrium for reaction j. The saturation index ($\mathrm{SI}_j = \log(\mathrm{IAP}_j/K_{eq,j})$) indicates the direction of mineral reactions, with positive values reflecting precipitation and negative values indicating dissolution. The code solves eq 1 for np primary species and n−np secondary species that participate in fast, equilibrium reactions. The primary species in the model were H^+, Ba^{2+}, Br^-, Ca^{2+}, Fe^{3+}, Mg^{2+}, SiO_2(aq), Na^+, Sr^{2+}, Zn^{2+}, SO_4^{2-}, Cl^-, and HCO_3^-. Secondary species were NaCl(aq), $CaCl^+$, $MgCl^+$, $BaCl^+$, $SrCl^+$, CO_3^{2-}, and CO_2(aq). The code considers mineral precipitation reactions as kinetic-controlled and aqueous complexation reactions as thermodynamic-controlled. Even though the mineral precipitation is considered kinetically controlled, the solubility/thermodynamic limits of $Ba_xSr_{1-x}SO_4$ precipitation controlled the predicted final concentrations. Although time-course samples were collected daily, this sampling frequency undersampled the reaction kinetic features of these experiments. As such, the calibration of the kinetic constant to the data at the end of 2 days may underestimate the reaction rates. Therefore, we focus on thermodynamics relevant to the

https://dx.doi.org/10.1021/acs.est.9b07072
Environ. Sci. Technol. XXXX, XXX, XXX−XXX

formation of $Ba_xSr_{1-x}SO_4$ such that we do not overinterpret the inferred kinetic information from the model. Batch reactor volume and the initial chemistry of AMD and HFFF immediately after mixing were used to set up the model; the aqueous data and solid chemistry data from the mixing experiments were used to calibrate the model. Equilibrium constants of tertiary mineral precipitates, with the general formula $Ba_xSr_{1-x}SO_4$ (Table S3), were included in CrunchFlow databases based on previous works.[23,24,46] Comparisons of best fit between laboratory experiments and theoretical total removal efficiencies calibrated the mineral formulas utilized in further modeling.

Under the constant temperature and pressure conditions in the mixing experiments, the thermodynamic limits of the precipitates (in the form of $Ba_xSr_{1-x}SO_4$) ultimately depend on two factors. One is salinity because of the high ion content in AMD and HFFF. The other is the value of x that quantifies the Ba content. Generally, the solubility of barite ($\log K_{eq} = -8.43$) is more than 2 orders of magnitude lower than that of celestite ($\log K_{eq} = -5.17$). To calculate the solubility of $Ba_xSr_{1-x}SO_4$, we followed the approach outlined in Rushdi et al. (2000), which considers $Ba_xSr_{1-x}SO_4$ solubility influenced by three factors: temperature, salinity, and Sr content. The salinity effects were included by calculating the activity coefficients (eq 7 in Rushdi et al. (2000)), following the Pitzer Formalism and ion-pairing model.[47−50] These activity coefficients were then used in eq 19 in Rushdi et al. (2000) to estimate equilibrium constants based on the Sr substitution approach (see the Supporting Information). Equilibrium constants estimated by this approach are consistent with those from approaches based on the solid solution theory.[51−53] Based on these estimations, we used $\log K_{eq}$ values of −8.42, −8.13, −7.53, −6.93 for $(Ba_{0.90}Sr_{0.10})SO_4$, $(Ba_{0.75}Sr_{0.25})SO_4$, $(Ba_{0.50}Sr_{0.50})SO_4$, and $(Ba_{0.25}Sr_{0.75})SO_4$, respectively.

RESULTS AND DISCUSSION

AMD and HFFF Fluid Characterization. Bituminous AMD sites A−D had wide-ranging SO_4 concentrations from 293 to 3873 mg/L (Table 1). From the previous work, four anthracite AMD sites were sampled from northeastern Pennsylvania and had lower SO_4 concentrations ranging from 53 to 175 mg/L.[43,44] Differences in SO_4 concentrations between anthracite and bituminous regions, important for co-treatment site selection, have been previously reported in Pennsylvania and are a function of season, mine hydrology, and time since mining operations.[20]

Because the four anthracite AMD sites were below, or just above, the industry proposed 100 mg/L SO_4 hydraulic fracturing cutoff limit for water utilization, this study focused only on the bituminous AMD sites with SO_4 concentrations >200 mg/L (Table 1). It should be noted that the proposed 100 mg/L SO_4 cutoff limit for hydraulic fracturing water utilization may still lead to some mineral precipitation in the O&G reservoir due to reaction with Ba concentrations in situ. Thus, utilizing AMD with SO_4 concentrations <200 mg/L or treating HFFF with AMD <100 mg/L SO_4 may be worthwhile moving forward if water recycling for use in hydraulic fracturing is the treatment goal.

HFFF samples had high TDS concentrations, which slightly increased, for most constituents, from early to late production (Table 1). Sample Well 1L had significantly more Ba than Sr with a Ba/Sr molar ratio of 2.3, whereas sample Well 2L had significantly less Ba than Sr with a Ba/Sr ratio of 0.2. Comparing the two, Well 1 had six times more Ba than Well 2, while Well 2 had 2 times more Sr. The HFFF compositions fall within ranges reported for produced water from Marcellus shale gas wells and reflect the variability between wells drilled in the same O&G formation within a similar geographic region.[54] Well 1 had higher Fe concentrations than Well 2 HFFF, while Well 2 Ca and Mg concentrations were more than double those in Well 1. The presence of other cations, such as Na and Ca, is important with regards to inhibition of barite and celestite precipitation kinetics through lattice growth poisoning.[24,55]

For the effects of organics, He et al. (2014) reported that TOC concentrations of 52 mg/L do not impact barite precipitation kinetics, likely increase barite solubility as previous studies also demonstrated, and decrease celestite precipitation kinetics.[24,56,57] In this study, Well 1E has TOC concentrations 5.4 times higher than Well 2E (180 vs 33 mg/L). We did not explicitly include the effects of organics on mineral precipitation in the model. However, the model was calibrated to actual measurements of Ba and Sr, which implicitly included the effects of TOC upward of 180 mg/L. Additionally, previous studies have indicated increased barite solubility, upward of 3 times, in the presence of organic matter that cannot be sufficiently incorporated in models, which typically overestimate Ba removal.[24,56,57] Due to the model overestimation of barite precipitation, laboratory data is vital for mixing ratio optimization calibration.

Kinetic Mixing Experiments and Mineral Precipitate Analysis to Calibrate the Model. From exploratory mixing experiments based on a 1:1 molar ratio of SO_4:Ba + Sr, ideal scenarios for the kinetic mixing experiment were selected (Table 2) and major and trace element data are presented in Table S4. Based on time-course samples (Figures 2 and 3, Table S5), 100% of Ba was removed for all but two AMD−HFFF mixtures (C + 2L with 70% Ba removal and B + 2L with 73% Ba removal) (Table 2). Both mixtures also had among the lowest total removals of Ba + Sr + SO_4 and the lowest SO_4:Ba + Sr molar ratios of the time-course experiments (0.15 and 0.20, respectively). The maximum total removal of Ba + Sr + SO_4 in this study was 80%, for mixture A + 1E, which occurred with the highest initial barite SI and approximate 1:1 molar ratios of both SO_4:Ba + Sr and SO_4:Ba. However, for this same mixture, individual removals of Sr and SO_4 were only 53 and 74%, respectively. Mixture D + 2E, which had the lowest initial barite SI of 1.8 and one of the highest AMD:HFFF mix ratios of 92%:8%, produced among the least total removal of Ba + Sr + SO_4 at 20%. Despite overall low total removal efficiency, Ba removal still remained high at 93%.

Batch mixing experiments indicated that there was little additional precipitation of minerals after 1 day of mixing. While true equilibrium may not have been achieved within 2 days (e.g., Sr increases slightly in some mixtures with longer residence time due to potential isomorphic substitution of Ba into celestite[24]), total removals were complete within 2 days. These results are promising for industry application of AMD−HFFF co-treatment as shorter residence times would decrease the size of infrastructure and, ultimately, cost.

Overall, best Ba (~100%) and Sr (~50%) removal occurred at 1:1 mol equiv SO_4:Ba+ Sr mixes. Best SO_4 removal occurred at ratios of 1:1 mol equiv of SO_4:Ba due to lack of sulfate precipitation when Ba is completely removed and did not depend on Sr concentrations. These results provide important insight into the reuse of AMD−HFFF mixtures to avoid

https://dx.doi.org/10.1021/acs.est.9b07072
Environ. Sci. Technol. XXXX, XXX, XXX−XXX

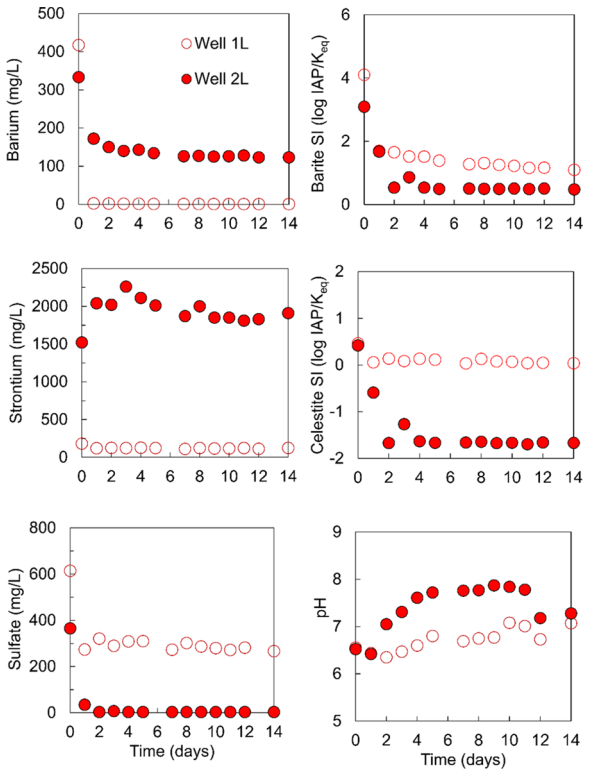

Figure 2. Fourteen day laboratory results for the mixture B + 1L at a 91%:9% AMD/HFFF volumetric ratio to achieve a 1:1 molar ratio of SO_4:Ba + Sr. Mixture B + 2L was mixed at a volumetric ratio of 54%:46% to achieve an approximate 1:1 molar ratio of SO_4:Ba. The results for Ba, Sr, and SO_4 are shown for each experiment. Note that in experiments where Ba has been completely removed from solution, Sr and SO_4 still remain dissolved. However, when SO_4 has been completely removed from solution, both Ba and Sr remain dissolved. Sr is never totally removed from solution. Even though Ba is consistently removed from solution, celestite SI continues to decrease with time.

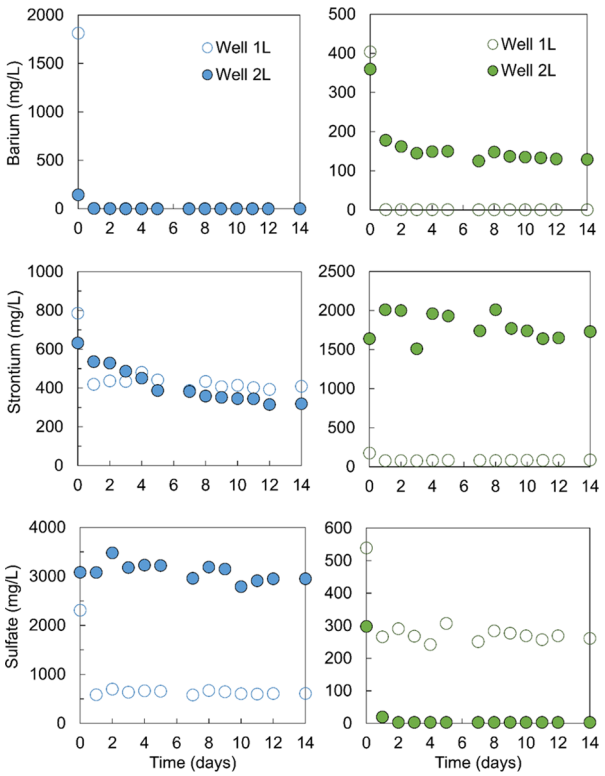

Figure 3. Fourteen day laboratory results for AMD site A (in blue) and AMD site C (in green). A + 1L and C + 1L were mixed at differing volumetric ratios of AMD/HFFF to achieve a 1:1 molar ratio of SO_4:Ba + Sr (60%:40% and 91%:9%, respectively). A + 2L was mixed to achieve a 1:1 molar ratio of SO_4:Ba + (4*Sr). C + 2L was mixed to achieve a 1:1 molar ratio of SO_4:Ba.

reinjecting residual sulfate into O&G formations where precipitation could occur with resident Ba.

XRD analysis of mineral precipitates did not detect celestite ($SrSO_4$) in samples collected after 14 days, even in the presence of residual SO_4 and Sr concentrations. Instead, XRD-detected Sr co-precipitated with Ba in the form $Ba_xSr_{1-x}SO_4$, while the most common minerals detected were $Ba_{0.75}Sr_{0.25}SO_4$, $BaSO_4$ and NaCl (Table S6). NaCl presence was likely a function of AMD−HFFF fluid in the pore water of the precipitated solids, which precipitated NaCl during drying prior to XRD analysis. No carbonate minerals ($SrCO_3$ or $CaCO_3$) were detected by XRD though pH did increase to 7.8 in two of the reactors, and SI for both minerals in all mixtures indicated supersaturation (Figure S1). To promote carbonate precipitation of Sr and inhibiting Ca presence, as suggested in previous studies,[58] use of high alkalinity lime-treated AMD remains a potential option for enhanced alkaline-earth metal removal from HFFF.

Model Extrapolation for Maximum Removal Efficiency AMD−HFFF Mixing Ratios. From both lab data and XRD analysis of precipitates, the CrunchFlow model was calibrated utilizing varying proportions of x within the $Ba_xSr_{1-x}SO_4$ formula. An example of the mineral and kinetic calibration can be seen in Figure 4 where removal efficiencies from lab data were best-matched to $(Ba_{0.75}Sr_{0.25})SO_4$, $(Ba_{0.50}Sr_{0.50})SO_4$, and $(Ba_{0.90}Sr_{0.10})SO_4$ and then applied to the time series of Ba, Sr, and SO_4 concentrations. Best-matched $Ba_xSr_{1-x}SO_4$ proportions from the model sweep-represented mixing experiments are presented in Table S7. The proportions of Ba and Sr in the mineral precipitate ultimately depend on the Ba/Sr molar ratio of the initial HFFF. For Ba/Sr molar ratios >1, the value of x was 0.75 or greater, while Ba/Sr molar ratios <1 contained compositions of x = 0.50 or less.

Figure 5a represents the general 1:1 relationship between Ba + Sr removed as a function of SO_4 removed during AMD−HFFF mixing experiments. All but two of the experiments exhibit stoichiometric removal of all species through the co-precipitation of strontian barite. A + 1E (SO_4:Ba + Sr = 0.98) falls above the 1:1 relationship, indicating higher removal of Ba + Sr relative to SO_4, whereas A + 1L (SO_4:Ba + Sr = 1.24) falls below the 1:1 line. The deviations from the 1:1 relationship could indicate minor precipitation (below XRD detection of <5% composition) of additional sulfate (e.g., $CaSO_4$) or carbonate (e.g., $SrCO_3$) minerals. Figure 5b demonstrates a strong positive logarithmic relationship between total removal efficiency (Ba + Sr + SO_4) and the initial SI of $BaSO_4$ in the AMD−HFFF mixtures. Higher values of $BaSO_4$ SI led to higher total removal efficiencies.

The CrunchFlow code, calibrated with experimental data and end-product $Ba_xSr_{1-x}SO_4$ formulas (confirmed by XRD), was then used to run simulations for varied volumetric mixing ratios of AMD−HFFF from 10 to 90% (Figure 4). Based on the model results, removal efficiency can be maximized at unique mixing ratios for each pair of AMD + HFFF (Figure 6).

https://dx.doi.org/10.1021/acs.est.9b07072
Environ. Sci. Technol. XXXX, XXX, XXX−XXX

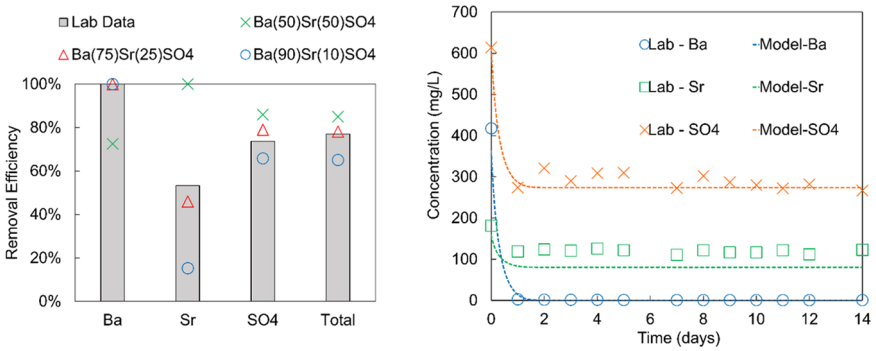

Figure 4. Example of calibrating model output removal efficiencies (Ba, Sr, SO_4, and total (Ba + Sr + SO_4)) with laboratory batch reactor-determined removal efficiencies (gray bars) with the optimum compositions of Ba and Sr in $Ba_xSr_{1-x}SO_4$ (left). 75 and 25%, respectively, were chosen to be the best composition representatives of the final batch mixing test precipitates, confirmed by the XRD results and plotted as concentrations versus time for B + 1L (right).

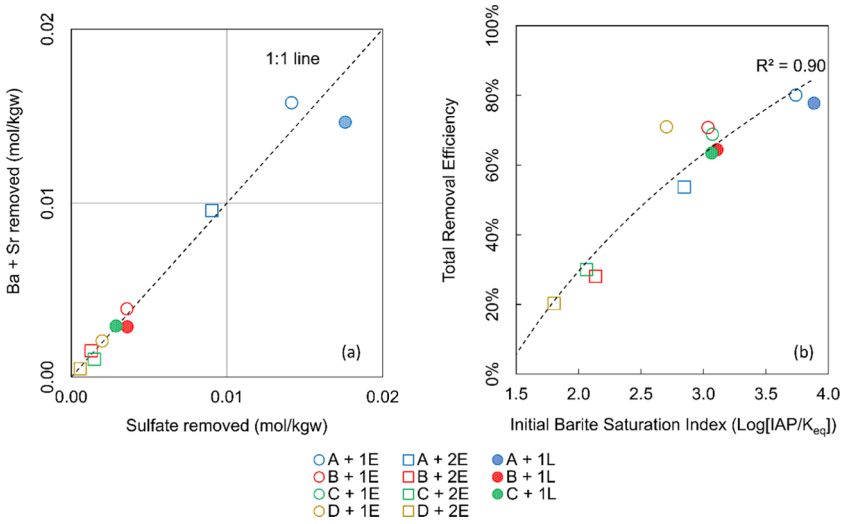

Figure 5. (a) Ba + Sr removal versus sulfate removal. The 1:1 line denotes stoichiometric removal of strontian barite. Dots below the 1:1 line indicate more removal of sulfate than Ba and Sr. Dots above the 1:1 line indicate more removal of Ba and Sr than SO_4. (b) Total removal efficiency versus initial $BaSO_4$ saturation index.

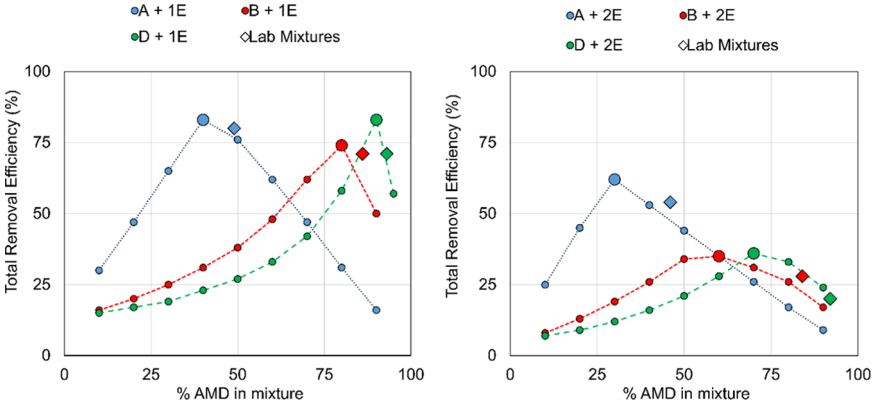

Figure 6. Geochemical model results for total removal efficiency (Ba + Sr + SO_4) versus volumetric % AMD in the mixture for (a) AMD sites + Well 1E and (b) AMD sites + Well 2E. The model results shown as lines with small symbols and large circles at the modeled optimum mixing ratio. The experimental results are shown as large diamonds. The modeled results show the percentage of AMD required to achieve the potential maximum total removal efficiencies, which can be applied to any initial solution chemistry to optimize treatment mixtures. Note that AMD mixtures with Well 1 had the highest optimum total removal efficiencies greater than or equal to 75% compared to Well 2 mixtures. Well 1 had a significantly higher initial Ba/Sr ratio than Well 2, which contributes to higher total removal efficiencies.

The AMD−HFFF ratios for optimum removal of Ba + Sr + SO_4 are directly affected by the SO_4 concentration in the AMD and the Ba and Sr concentrations in the HFFF. Because these concentrations in AMD samples A, B, and C and samples Well 1E and Well 2E (all paired simulations shown in Figure 6) all varied, optimum total removal efficiencies were always

https://dx.doi.org/10.1021/acs.est.9b07072
Environ. Sci. Technol. XXXX, XXX, XXX−XXX

achieved as some unique volumetric mixing ratio. Because of the high sulfate concentration of AMD sample A, maximum removal efficiencies for the mixtures A + 1E and A + 2E could be achieved at lower volumetric mixing ratios of AMD−HFFF as compared to AMD samples B and D. Because of the higher concentrations of Ba and Sr in sample Well 1E, maximum removal efficiencies for mixtures with all three AMD samples were always higher with Well 1E as compared to Well 2E.

Well 1 HFFF mixing yielded relatively consistent maximum removal efficiencies between 75 and 85% due to higher Ba concentrations compared to Well 2. Thus, high Ba concentrations in HFFF are required initially to efficiently remove Ba, Sr, and SO_4 from solution. Ba concentrations in HFFF ultimately control total removal efficiency, while AMD vol % of mixtures can be adjusted using the model developed in this study to achieve the ideal SO_4:Ba ratio. It is important to note here that Well 1E HFFF-optimized mixing ratios lead to higher total ion removal than Well 2E HFFF even though TOC concentrations in Well 1 HFFF were 5.4 times higher, further evincing the initial Ba concentrations as a controlling mechanism.

Potential Beneficial Uses of AMD−HFFF-Treated Fluids With Regards to Radium Removal. Consistent with the previous work indicating that AMD−HFFF mixing provides significant Ra removal,[32,58,59] Ra removals for three AMD−HFFF mixtures were >96% for Ra-226 and >82% for Ra-228, leading to the highest remnant total Ra concentration in a treated fluid of approximately 44 pCi/L (Table 2). This value is less than the 60 pCi/L EPA National Pollutant Discharge Elimination System (NPDES) standard for disposal of treated HFFF to surface water. Ouyang et al. (2019) and Ouyang (2019) analyzed the solid precipitates from this study's mixing experiments and found that 80−97% of the Ra-226 was associated with sulfate minerals and that higher specific Ra-226 sequestration increased with increasing Sr/Ba ratios of the initial AMD−HFFF mixture.[59,60] This is important with regards to Ra treatment due to the ability to adjust Sr/Ba ratios to concentrate more Ra into a smaller mass of precipitate for subsequent landfill disposal. From previous studies, Ra readily co-precipitates into binary or ternary solid solutions such as $(Ba,Ra)SO_4$ and $(Ba,Sr,Ra)SO_4$, which were not modeled in this study.[12,36−38,61] Zhang et al. (2014) and Rosenberg et al. (2018) found that co-precipitation of $(Ba,Ra)SO_4$ could also explain Ra removal behavior.[32,62] The AMD−HFFF mixtures in this study had partition coefficients for Ra incorporation within celestite (250−1700) 2 magnitudes greater compared to barite (1.7−11.3).[59] Calculated SI values for celestite either remained steady or decreased with time (Figures 2 and S2) even though the Sr/Ba molar ratio steadily increased as Ba precipitated from the mixture. Furthermore, literature discrepancies exist where decreasing Sr/Ba ratios (in the range of 0−1)[32,63] and increasing Sr/Ba ratios (in the range of 10−10 000)[64] increase Ra removal, with no data for Sr/Ba ratios between 1 and 10. In this study, initial Sr/Ba ratios were approximately 0.7 and 7 and resulted in diverging specific Ra activities (Bq/g) in the solids, with the higher initial Sr/Ba ratios of 7 leading to the highest average specific Ra activity and lowest average mass of the precipitate.[59] This result is significant due to the inverse trend in maximizing the total removal of Ba + Sr + SO_4 with lower Sr/Ba ratios (Figure S3). From charge-balanced Pennsylvania conventional and unconventional USGS Produced Water Database samples,[65] Sr/Ba ratios range widely from 0.1 to above 1000. Mixing ratios for initial Sr/Ba ratios in AMD−HFFF can be adjusted depending on the ultimate treatment agenda. For example, if AMD−HFFF treatment is intended for reuse in hydraulic fracturing, decreasing the initial mixture Sr/Ba molar ratio is necessary to maximize Ba + Sr + SO_4 removal to avoid remnant SO_4 concentrations reinjected into the formation. If AMD−HFFF treatment (with similar ratios presented in this study) is intended for recycling water for agriculture, dust suppression, or road deicing, increasing the initial Sr/Ba molar ratio maximizes Ra concentration into a smaller mass that is more cost effective to landfill and creates a near Ra-free fluid that can be beneficially used. A hybrid of both treatment agendas can also be defined.

At the time of publication, Tasker et al. (2018) identified 13 U.S. states that utilized conventional O&G wastewater for dust suppression and deicing, targeting high TDS brines enriched in Ca and Mg.[66,67] Conventional- and unconventional produced waters share similar inorganic chemistry.[65] While HFFF samples were utilized in this study, the developed CrunchFlow code can be applied to both conventional and unconventional produced waters. Michigan did not differentiate between the allowable use of unconventional versus conventional produced water on roads until 2012.[68] In a regulatory survey of a subset of states that allowed road spreading, only oil−water separation was required prior to spreading or no treatment.[68] Ra was not monitored in brines of states surveyed, and New York and North Dakota were the only states to monitor lead and arsenic concentrations. Over 60 million liters of conventional produced water were road spread for dust suppression in 2012 in Pennsylvania.[66] If road maintenance is the desired treatment outcome for produced waters, operators can utilize the malleable Sr/Ba ratios for secondary treatment that maximizes Ra removal and, from this study, reduces arsenic concentrations between 4 and 20 times and reduces lead concentrations between 33 and 100 times. Ca concentrations remained high throughout batch experiments (Figure S1), indicating fluids with good potential for dust suppression. In some O&G regions, such as Wyoming, produced water with high sulfate concentrations and relatively low Ba and Sr concentrations is recycled for agriculture.[28,30,69] Our results suggest that adding preformed barite mineral seed to existing infrastructure could decrease the Sr/Ba ratio and induce maximum mass removals of Ba + Sr + SO_4, creating a recycled fluid more appropriate for agricultural end-use.

Environmental Implications of Optimizing Energy Waste Stream Mixing for Beneficial Use. AMD discharges from the bituminous coal region of Pennsylvania remain a viable treatment candidate when mixed with HFFF prior to water recycling for stimulation of shale gas wells or other beneficial reuses. While Ba can be removed completely at molar ratios of 1:1 (SO_4:Ba + Sr) within 1 day of mixing, Sr and SO_4 concentrations remaining after 14 days appear dependent on the Ba/Sr ratio of the initial HFFF. When Ba is depleted, Sr will not be removed without the potential addition of alkalinity for alternative mineral precipitation (beyond the scope of this study). XRD analysis confirmed that celestite did not form; rather, Sr co-precipitated with Ba in the form of $Ba_xSr_{1-x}SO_4$ where x depends on the Ba/Sr ratio of the HFFF. With data obtained in this study, an open-source geochemical code predicts optimal mix ratios to remove Ba and SO_4 in the mix and is now available in the SI for regulators and operators. This optimum volumetric mix ratio depends on the initial HFFF-Ba concentration, whereas the maximum

https://dx.doi.org/10.1021/acs.est.9b07072
Environ. Sci. Technol. XXXX, XXX, XXX−XXX

removal efficiency is a function of initial Ba and SO_4 concentrations, or $BaSO_4$ SI. AMD-SO_4 concentrations, ranging from low to high, could achieve the same total maximum removal efficiencies when Ba concentrations from initial HFFF were high at AMD−HFFF mix ratios determined from the model. Further, this study sheds light on the diverging potential process flow pathway for management decisions regarding beneficial uses of AMD−HFFF co-treated fluids. High initial fluid Sr/Ba molar ratios (approximately >10) can lead to optimized treatment for Ra removal, generating a small mass of highly concentrated radioactive precipitates that would be more cost effective to landfill and a nearly Ra-free fluid. Low initial Sr/Ba molar ratios (approximately <1) can lead to optimized treatment for the total removal of Ba + Sr + SO_4, generating a large mass of precipitates, including Ra, and a fluid that would be more applicable for use in hydraulic fracturing water recycling.

■ ASSOCIATED CONTENT

Supporting Information

The Supporting Information is available free of charge at https://pubs.acs.org/doi/10.1021/acs.est.9b07072.

Reaction modeling with CrunchFlow; 14 day batch mixing experiment results are presented for AMD sites A, B, and C (PDF)

AMD major and trace element chemistry full dataset; HFFF major and trace element chemistry dataset; exploratory fourteen day AMD−HFFF mixtures major and trace element chemistry (PDF)

CrunchFlow code example and database (PDF)

■ AUTHOR INFORMATION

Corresponding Author

Bonnie McDevitt − *Department of Civil and Environmental Engineering, The Pennsylvania State University, University Park, Pennsylvania 16802, United States;* orcid.org/0000-0001-8390-0028; Email: bum49@psu.edu

Authors

Michael Cavazza − *Department of Energy and Mineral Engineering, The Pennsylvania State University, University Park, Pennsylvania 16802, United States*

Richard Beam − *Pennsylvania Department of Environmental Protection, Bureau of Abandoned Mine Reclamation, Ebensburg, Pennsylvania 15931, United States*

Eric Cavazza − *Pennsylvania Department of Environmental Protection, Bureau of Abandoned Mine Reclamation, Harrisburg, Pennsylvania 17106, United States*

William D. Burgos − *Department of Civil and Environmental Engineering, The Pennsylvania State University, University Park, Pennsylvania 16802, United States;* orcid.org/0000-0003-3269-2921

Li Li − *Department of Civil and Environmental Engineering, The Pennsylvania State University, University Park, Pennsylvania 16802, United States;* orcid.org/0000-0002-1641-3710

Nathaniel R. Warner − *Department of Civil and Environmental Engineering, The Pennsylvania State University, University Park, Pennsylvania 16802, United States;* orcid.org/0000-0002-6434-5118

Complete contact information is available at: https://pubs.acs.org/10.1021/acs.est.9b07072

Author Contributions

The manuscript was written through the contributions of all authors. All authors have given approval to the final version of the manuscript.

Notes

The authors declare no competing financial interest.

■ ACKNOWLEDGMENTS

A special thanks to the Pennsylvania Department of Environmental Protection for their time and effort in ensuring the completion of this project. This project was partially funded by the National Energy Technology Laboratory (NETL), U.S. Department of Energy, an agency of the United States Government, through a support contract through Project RES1000026 with URS Energy and Construction, Inc. Funding for B.M. came from The Pennsylvania State University and NSF grant 1703412. Dr. Radisav Vidic of the University of Pittsburgh deserves recognition for the foundation of this research and should be acknowledged for his help in the creation of this project. M.C. would also thank Tom Gray and Terry Smith, of TetraTech, for their instrumental role in pursuing this research topic.

■ REFERENCES

(1) EIA. *Appalachia Region Drilling Productivity Report*; 2019.

(2) U.S. Energy Information Administration. Natural Gas. https://www.eia.gov/naturalgas/reports.php#/T202,T1075 (accessed Oct 9, 2019).

(3) PASDA. Pennsylvania Spatial Data Access. https://www.pasda.psu.edu/.

(4) Vengosh, A.; Jackson, R. B.; Warner, N.; Darrah, T. H.; Kondash, A. A Critical Review of the Risks to Water Resources from Unconventional Shale Gas Development and Hydraulic Fracturing in the United States. *Environ. Sci. Technol.* **2014**, *48*, 8334−8348.

(5) Scanlon, B. R.; Reedy, R. C.; Nicot, J. P. Will Water Scarcity in Semiarid Regions Limit Hydraulic Fracturing of Shale Plays? *Environ. Res. Lett.* **2014**, *9*, No. 124011.

(6) Lauer, N.; Vengosh, A. Age Dating Oil and Gas Wastewater Spills Using Radium Isotopes and Their Decay Products in Impacted Soil and Sediment. *Environ. Sci. Technol. Lett.* **2016**, *3*, 205−209.

(7) Lauer, N. E.; Warner, N. R.; Vengosh, A. Sources of Radium Accumulation in Stream Sediments near Disposal Sites in Pennsylvania: Implications for Disposal of Conventional Oil and Gas Wastewater. *Environ. Sci. Technol.* **2018**, *52*, 955−962.

(8) Cozzarelli, I. M.; Skalak, K. J.; Kent, D. B.; Engle, M. A.; Benthem, A.; Mumford, A. C.; Haase, K.; Farag, A.; Harper, D.; Nagel, S. C.; Iwanowicz, L. R.; Orem, W. H.; Akob, D. M.; Jaeschke, J. B.; Galloway, J.; Kohler, M.; Stoliker, D. L.; Jolly, G. D. Environmental Signatures and Effects of an Oil and Gas Wastewater Spill in the Williston Basin, North Dakota. *Sci. Total Environ.* **2017**, *579*, 1781−1793.

(9) Shrestha, N.; Chilkoor, G.; Wilder, J.; Gadhamshetty, V.; Stone, J. J. Potential Water Resource Impacts of Hydraulic Fracturing from Unconventional Oil Production in the Bakken Shale. *Water Res.* **2017**, *108*, 1−24.

(10) Kondash, A. J.; Lauer, N. E.; Vengosh, A. The Intensification of the Water Footprint of Hydraulic Fracturing. *Sci. Adv.* **2018**, *4*, No. eaar5982.

(11) Gregory, K. B.; Vidic, R. D.; Dzombak, D. A. Water Management Challenges Associated with the Production of Shale Gas by Hydraulic Fracturing. *Elements* **2011**, *7*, 181−186.

(12) Van Sice, K.; Cravotta, C. A.; McDevitt, B.; Tasker, T. L.; Landis, J. D.; Puhr, J.; Warner, N. R. Radium Attenuation and Mobilization in Stream Sediments Following Oil and Gas Wastewater Disposal in Western Pennsylvania. *Appl. Geochem.* **2018**, *98*, 393−403.

https://dx.doi.org/10.1021/acs.est.9b07072
Environ. Sci. Technol. XXXX, XXX, XXX−XXX

(13) Geeza, T. J.; Gillikin, D. P.; McDevitt, B.; Van Sice, K.; Warner, N. R. Accumulation of Marcellus Formation Oil and Gas Wastewater Metals in Freshwater Mussel Shells. *Environ. Sci. Technol.* **2018**, *52*, 10883−10892.
(14) Burgos, W. D.; Castillo-Meza, L.; Tasker, T. L.; Geeza, T. J.; Drohan, P. J.; Liu, X.; Landis, J. D.; Blotevogel, J.; McLaughlin, M.; Borch, T.; Warner, N. R. Watershed-Scale Impacts from Surface Water Disposal of Oil and Gas Wastewater in Western Pennsylvania. *Environ. Sci. Technol.* **2017**, *51*, 8851−8860.
(15) Wilson, J. M.; Vanbriesen, J. M. Oil and Gas Produced Water Management and Surface Pennsylvania. *Environ. Pract.* **2012**, *14*, 288−301.
(16) Akob, D. M.; Mumford, A. C.; Orem, W.; Engle, M. A.; Klinges, J. G.; Kent, D. B.; Cozzarelli, I. M. Wastewater Disposal from Unconventional Oil and Gas Development Degrades Stream Quality at a West Virginia Injection Facility. *Environ. Sci. Technol.* **2016**, *50*, 5517−5525.
(17) Kassotis, C. D.; Iwanowicz, L. R.; Akob, D. M.; Cozzarelli, I. M.; Mumford, A. C.; Orem, W. H.; Nagel, S. C. Endocrine Disrupting Activities of Surface Water Associated with a West Virginia Oil and Gas Industry Wastewater Disposal Site. *Sci. Total Environ.* **2016**, *557*−*558*, 901−910.
(18) Pennsylvania Department of Environmental Protection. 2014 Pennsylvania Integrated Water Quality Monitoring and Assessment Report, 2014, Vol. *2014*.
(19) Pennsylvania Department of Environmental Protection. Acid Mine Drainage Set-Aside Program Implementation Guidelines, 2015.
(20) Cravotta, C. A. Dissolved Metals and Associated Constituents in Abandoned Coal-Mine Discharges, Pennsylvania, USA. Part 1: Constituent Quantities and Correlations. *Appl. Geochem.* **2008**, *23*, 166−202.
(21) Growitz, B. D. J.; Reed, L. A.; Beard, M. M. Survey, U. S. G. Reconnaissance of Mine Drainage in the Coal Fields of EasternPennsylvania; Harrisburg, 1985. https://doi.org/10.3133/wri834274.
(22) Curtright, A. E.; Giglio, K. Coal Mine Drainage for Marcellus Shale Natural Gas Extraction, 2012.
(23) Kondash, A. J.; Warner, N. R.; Lahav, O.; Vengosh, A. Radium and Barium Removal through Blending Hydraulic Fracturing Fluids with Acid Mine Drainage. *Environ. Sci. Technol.* **2014**, *48*, 1334−1342.
(24) He, C.; Li, M.; Liu, W.; Barbot, E.; Vidic, R. D. Kinetics and Equilibrium of Barium and Strontium Sulfate Formation in Marcellus Shale Flowback Water. *J. Environ. Eng.* **2014**, *140*, B4014001-1−B4014001-9.
(25) Wang, Y.; Tavakkoli, S.; Khanna, V.; Vidic, R. D.; Gilbertson, L. M. Life Cycle Impact and Benefit Trade-Offs of a Produced Water and Abandoned Mine Drainage Cotreatment Process. *Environ. Sci. Technol.* **2018**, *52*, 13995−14005.
(26) Coonrod, C. L.; Yin, Y. B.; Hanna, T.; Atkinson, A.; Alvarez, P. J. J.; Tekavec, T. N.; Reynolds, M. A.; Wong, M. S. Fit-for-Purpose Treatment Goals for Produced Waters in Shale Oil and Gas Fields. *Water Res.* **2020**, *173*, No. 115467.
(27) EPA.Study of Oil and Fas Extraction Wastewater Management.https://www.epa.gov/eg/study-oil-and-gas-extraction-wastewater-management.
(28) McDevitt, B.; Mclaughlin, M.; Cravotta, C. A.; Ajemigbitse, M. A.; Van Sice, K. J.; Blotevogel, J.; Borch, T.; Warner, N. R. Emerging Investigator Series: Radium Accumulation in Carbonate River Sediments at Oil and Gas Produced Water Discharges: Implications for Beneficial Use as Disposal Management. *Environ. Sci.: Processes Impacts* **2019**, *21*, 324−338.
(29) McLaughlin, M.; Borch, T.; McDevitt, B.; Warner, N. R.; Blotevogel, J. Water Quality Assessment Downstream of Oil and Gas Produced Water Discharges Intended for Beneficial Reuse in Arid Regions. *Sci. Total Environ.* **2020**, *713*, No. 136607.
(30) McDevitt, B.; McLaughlin, M.; Vinson, D. S.; Geeza, T. J.; Blotevogel, J.; Borch, T.; Warner, N. R. Isotopic and Element Ratios Fingerprint Salinization Impact from Beneficial Use of Oil and Gas Produced Water in the Western U.S. *Sci. Total Environ. 716*, 137006. DOI: 10.1016/j.scitotenv.2020.137006.
(31) Zhang, T.; Hammack, R. W.; Vidic, R. D. Fate of Radium in Marcellus Shale Flowback Water Impoundments and Assessment of Associated Health Risks. *Environ. Sci. Technol.* **2015**, *49*, 9347−9354.
(32) Zhang, T.; Gregory, K.; Hammack, R. W.; Vidic, R. D. Co-Precipitation of Radium with Barium and Strontium Sulfate and Its Impact on the Fate of Radium during Treatment of Produced Water from Unconventional Gas Extraction. *Environ. Sci. Technol.* **2014**, *48*, 4596−4603.
(33) Grandia, F.; Merino, J.; Bruno, J. Assessment of the Radium-Barium Co-Precipitation and Its Potentialinfluence on the Solubility of Ra in the near-Field. Technical Report TR-08-07, 2008, p 52.
(34) Langmuir, D.; Melchior, D. The Geochemistry of Ca, Sr, Ba and Ra Sulfates in Some Deep Brines from the Palo Duro Basin, Texas. *Geochim. Cosmochim. Acta* **1985**, *49*, 2423−2432.
(35) Brandt, F.; Curti, E.; Klinkenberg, M.; Rozov, K.; Bosbach, D. Replacement of Barite by a (Ba,Ra)SO4 Solid Solution at Close-to-Equilibrium Conditions: A Combined Experimental and Theoretical Study. *Geochim. Cosmochim. Acta* **2015**, *155*, 1−15.
(36) Vinograd, V. L.; Brandt, F.; Rozov, K.; Klinkenberg, M.; Refson, K.; Winkler, B.; Bosbach, D. Solid-Aqueous Equilibrium in the BaSO4-RaSO4-H2O System: First-Principles Calculations and a Thermodynamic Assessment. *Geochim. Cosmochim. Acta* **2013**, *122*, 398−417.
(37) Vinograd, V. L.; Kulik, D. A.; Brandt, F.; Klinkenberg, M.; Weber, J.; Winkler, B.; Bosbach, D. Thermodynamics of the Solid Solution - Aqueous Solution System (Ba,Sr,Ra)SO4+ H2O: II. Radium Retention in Barite-Type Minerals at Elevated Temperatures). *Appl. Geochem.* **2018**, *93*, 190−208.
(38) Vinograd, V. L.; Kulik, D. A.; Brandt, F.; Klinkenberg, M.; Weber, J.; Winkler, B.; Bosbach, D. Thermodynamics of the Solid Solution - Aqueous Solution System (Ba,Sr,Ra)SO4 + H2O: I. The Effect of Strontium Content on Radium Uptake by Barite. *Appl. Geochem.* **2018**, *89*, 59−74.
(39) Paukert Vankeuren, A. N.; Hakala, J. A.; Jarvis, K.; Moore, J. E. Mineral Reactions in Shale Gas Reservoirs: Barite Scale Formation from Reusing Produced Water As Hydraulic Fracturing Fluid. *Environ. Sci. Technol.* **2017**, *51*, 9391−9402.
(40) PA DEP. WhitePaper: Utilization of AMD in Well Development for Natural Gas ExtractionEstablishment of a Process for the Oil and Gas Industry to Utilize AMD, 2011.
(41) Zhang, L.; Tice, M.; Hascakir, B. The Impact of Re-Injecting Flowback Fluids on Formation Damage. Case Study: Marcellus Shale. *SPE West. Reg. Meet. Proc.* **2019**, *2019*, 23−26.
(42) He, C.; Zhang, T.; Vidic, R. D. Co-Treatment of Abandoned Mine Drainage and Marcellus Shale Flowback Water for Use in Hydraulic Fracturing. *Water Res.* **2016**, *104*, 425−431.
(43) Cavazza, M. In Reducing Freshwater Consumption in the Marcellus Shale Play by Recycling Flowback with Acid Mine Drainage, Proceedings of the SPE Annual Technical Conference and Exhibition, January, Vol 2016, 2016.
(44) Cavazza, M. Reducing Freshwater Consumption in the Marcellus Shale Play by Recycling Flowback with Abandoned Mine Drainage. Ph.D. Thesis, The Pennsylvania State University, 2016.
(45) Steefel, C. I. CrunchFlow Software for Modeling Multi-component Reactive Flow and Transport User's Manual, 2009, p 91.
(46) He, C.; Zhang, T.; Vidic, R. D. Use of Abandoned Mine Drainage for the Development of Unconventional Gas Resources. *Disruptive Sci. Technol.* **2013**, *1*, 169−176.
(47) Millero, F. J. Chemical Speciation of Ionic Compounds in Estuarine Systems. *River Inputs to Ocean Systems*; UNEP/SCOR, 1981; pp 116−131.
(48) Millero, F. J. *The Physical Chemistry of Natural Waters*; Wiley-Interscience: New York, 2001.
(49) Millero, F. J.; Schreiber, D. R. Use of the Ion Pairing Model to Estimate Activity Coefficients of the Ionic Components of Natural Waters. *Am. J. Sci.* **1982**, *282*, 1508−1540.

https://dx.doi.org/10.1021/acs.est.9b07072
Environ. Sci. Technol. XXXX, XXX, XXX−XXX

(50) Rushdi, A. I.; McManus, J.; Collier, R. W. Marine Barite and Celestite Saturation in Seawater. *Mar. Chem.* **2000**, *69*, 19−31.
(51) Glynn, P. Solid-Solution Solubilities and Thermodynamics: Sulfates, Carbonates and Halides. *Rev. Mineral. Geochem.* **2000**, *40*, 481−511.
(52) Glynn, P.; Reardon, E. J. Solid-Solution Aqueous-Solution Equilibria: Thermodynamic Theory and Representation. *Am. J. Sci.* **1990**, *290*, 164−201.
(53) Prieto, M. Thermodynamics of Solid Solution Aqueous Solution Systems. *Rev. Mineral. Geochem.* **2009**, *70*, 47−85.
(54) Barbot, E.; Vidic, N. S.; Gregory, K. B.; Vidic, R. D. Spatial and Temporal Correlation of Water Quality Parameters of Produced Waters from Devonian-Age Shale Following Hydraulic Fracturing. *Environ. Sci. Technol.* **2013**, *47*, 2562−2569.
(55) Jones, F.; Oliviera, A.; Parkinson, G. M.; Rohl, A. L.; Stanley, A.; Upson, T. The Effect of Calcium Cations on the Precipitation of Barium Sulfate 2: Calcium Ions in the Presence of Organic Additives. *J. Cryst. Growth* **2004**, *270*, 593−603.
(56) Church, T. M.; Wolgemuth, K. Marine Barite Saturation. *Earth Planet. Sci. Lett.* **1972**, *15*, 35−44.
(57) Desai, M. V. M.; Koshy, E.; Ganguly, A. K. Solubility of Barium in Seawater in Presence of Dissolved Organic Matter. *Curr. Sci.* **1969**, *38*, 107−108.
(58) Kondash, A. J.; Warner, N. R.; Lahav, O.; Vengosh, A. Radium and Barium Removal through Blending Hydraulic Fracturing Fluids with Acid Mine Drainage. *Environ. Sci. Technol.* **2014**, *48*, 1334−1342.
(59) Ouyang, B.; Renock, D. J.; Ajemigbitse, M. A.; Van Sice, K.; Warner, N. R.; Landis, J. D.; Feng, X. Radium in Hydraulic Fracturing Wastewater: Distribution in Suspended Solids and Implications to Its Treatment by Sulfate Co-Precipitation. *Environ. Sci.: Processes Impacts* **2019**, *21*, 339−351.
(60) Ouyang, B. Radium,Strontium and Barium in Hydraulic Fracturing Wastewater − Distribution,Dissolution, and Co-Precipitation. Dartmouth College, 2019.
(61) Rodríguez-Galán, R. M.; Prieto, M. Interaction of Nonideal, Multicomponent Solid Solutions With Water: A Simple Algorithm to Estimate Final Equilibrium States. *Geochem., Geophys., Geosyst.* **2018**, *19*, 1348−1359.
(62) Rosenberg, Y. O.; Sade, Z.; Ganor, J. The Precipitation of Gypsum, Celestine, and Barite and Coprecipitation of Radium during Seawater Evaporation. *Geochim. Cosmochim. Acta* **2018**, *233*, 50−65.
(63) Ceccarello, S.; Black, S.; Read, D.; Hodson, M. E. Industrial Radioactive Barite Scale: Suppression of Radium Uptake by Introduction of Competing Ions. *Miner. Eng.* **2004**, *17*, 323−330.
(64) Goldschmidt, B. On Mixed Precipitation of Sulphates of Barium and Strontium. *C. R. Hebd. Seances Acad. Sci.* **1938**, *206*, 1110−1113.
(65) Blondes, M. S.; Gans, K. D.; Engle, M. A.; Kharaka, Y. K.; Reidy, M. E.; Saraswathula, V.; Thordsen, J. J.; Rowan, E. L.; Morrissey, E. A. U.S. Geological Survey National Produced Waters Geochemical Database (ver. 2.3, January 2018). https://doi.org/doi.org/10.5066/F7J964W8.
(66) Tasker, T. L.; Burgos, W. D.; Piotrowski, P.; Castillo-Meza, L.; Blewett, T. A.; Ganow, K. B.; Stallworth, A.; Delompré, P. L. M.; Goss, G. G.; Fowler, L. B.; Vanden Heuvel, J. P.; Dorman, F.; Warner, N. R. Environmental and Human Health Impacts of Spreading Oil and Gas Wastewater on Roads. *Environ. Sci. Technol.* **2018**, *52*, 7081−7091.
(67) Stallworth, A. M.; Chase, E. H.; Burgos, W. D.; Warner, N. R. *Laboratory Method to Assess Efficacy of Dust Supressants for Dirt and Gravel Roads*; Transportation Research Board, 2019.
(68) Goodman, C. BeneficialUse of Produced Water for Road-spreading: Perspectives for Colorado Policymakers; Denver, 2017. https://doi.org/10.1017/CBO9781107415324.004.
(69) McLaughlin, M. C.; Borch, T.; McDevitt, B.; Warner, N. R.; Blotevogel, J. Water Quality Assessment Downstream of Oil and Gas Produced Water Discharges Intended for Beneficial Reuse in Arid Regions. *Sci. Total Environ.* **2020**, *713*, No. 136607.

https://dx.doi.org/10.1021/acs.est.9b07072
Environ. Sci. Technol. XXXX, XXX, XXX−XXX